6.3 Comparing an urban metabolism model to long-term CO_2 eddy-covariance measurements

A. Christen[(1)]*, N. C. Coops[(2)], B. Crawford[(1)], R. Kellett[(3)], K. N. Liss[(1,4)], T. R. Oke[(1)], I. Olchovski[(3)], R. Tooke[(2)], M. van der Laan[(1,3)], and J. A. Voogt[(5)]

[(1)] Department of Geography, University of British Columbia, Vancouver, BC, Canada
[(2)] Forest Sciences, University of British Columbia, Vancouver, BC, Canada
[(3)] School of Architecture and Landscape Architecture, University of British Columbia, Vancouver, BC, Canada
[(4)] Center for Global Change Sciences, University of Toronto, Toronto, ON, Canada
[(5)] Department of Geography, University of Western Ontario, London, ON, Canada

Abstract – Carbon-dioxide (CO_2) emissions modeled using an urban metabolism approach are validated against direct eddy-covariance flux measurements. Model inputs include automated urban object classifications based on LiDAR, optical remote sensing, census data, assessment data, traffic counts and measured radiation and climate data to model net CO_2 emissions by buildings, transportation, human respiration, soils and vegetation. A primarily residential area of 4 km^2 in Vancouver, BC, Canada has been selected for a case-study. The area is chosen to overlap with the source-area of a micrometeorological flux tower for which continuous CO_2-flux data were available for a two-year period. Modeled and measured emissions agreed within 11% with 6.71 kg C m^{-2} $year^{-1}$ measured vs. 7.11 kg C m^{-2} $year^{-1}$ modeled, but show higher differences in wind sectors dominated by traffic emissions indicating that a more sophisticated transportation model is required. The study shows that direct CO_2 flux measurements from urban flux towers - if carefully sited - are a promising method to validate fine-scale emission inventories / models at the block or neighborhood scale.

Keywords – GHG emission modeling, building energy modeling, carbon-dioxide, flux measurements, eddy-covariance, LiDAR, model validation.

1 INTRODUCTION

1.1 Motivation of this study

As much as 50% of greenhouse-gas (GHG) emissions in cities are attributable to urban form choices - notably: density, land use mix, spatial patterns, building types, transportation networks, and vegetation. Salat (2007) and Baker and Steemers (2000), for example, argue that urban form variation can influence urban building energy demand by factors up to 2.5 and urban energy systems performance by factors up to 2.

As urban planning falls within the regulatory domain of governments, planning policy and regulation can promote urban form and transportation strategies to meet energy- and GHG emission-reduction targets. Appropriate models are required to evaluate the impact, and opportunity, of various future planning and design scenarios on all relevant components that emit or uptake GHGs in urban ecosystems – buildings, transportation, human metabolism, food and waste, soils, and vegetation.

A particular challenge has been an independent validation of urban emission models at fine scales (block, neighborhood). To date, model validation is done using consumption statistics that are available at coarser scales (consumption and utility statistics at the national, provincial, and municipal-level). Direct flux measurements of GHGs using micrometeorological methods are a promising approach to provide data for model validation at finer scales. Fluxes of carbon dioxide (CO_2) – the most relevant GHG in urban ecosystems, can be directly and continuously measured using the Eddy covariance (EC) method on towers above the urban surface of interest. In combination with source-area models, EC measurements provide spatial information that can be used to evaluate spatial patterns.

As flux measurements provide total CO_2 emitted, they cannot be used to validate sector-individual models (e.g. solely building energy models, transportation models).

1.2 Case study area

Here we discuss a case study where direct flux measurements integrated over two years were compared to an urban metabolism model. The modeled area is a primarily residential area of 1900 m by 1900 m in south central Vancouver, BC, Canada – centered on the EC tower 'Vancouver-Sunset' (494290, 5452601, UTM-10). Of the total plan area, 29% is building footprints, 11% is tree covered, 24% is uncovered ground vegetation and 35% is non-vegetated ground surfaces (streets, sidewalks, driveways). The majority of the population (23,166 Inh., 64.2 Inh./ha) lives in single-family residential dwellings. Within the study area are 4155 detached dwellings. Approximately 55% have secondary suites. Approximately 37% of residential dwellings were built before 1965, 38% between 1965 and 1990, and 25% post 1990. The area's commercial and higher density residential nodes and corridors are concentrated along few arterial streets. Three larger public parks cover 6% of study area.

2 NEIGHBORHOOD-SCALE EMISSION MODEL

2.1 The metabolism model concept

In the proposed urban metabolism approach, carbon is conceptually tracked through quantifying inputs and outputs into part of the urban subsystem (1900 x 1900m neighborhood), as well as storage changes within the system. Inputs and outputs can happen at different boundaries (lateral, vertical) and in different chemical forms (e.g. carbohydrates, CO_2). Vertical fluxes are fluxes at the system's upper boundary (land-atmosphere interface) and result from chemical

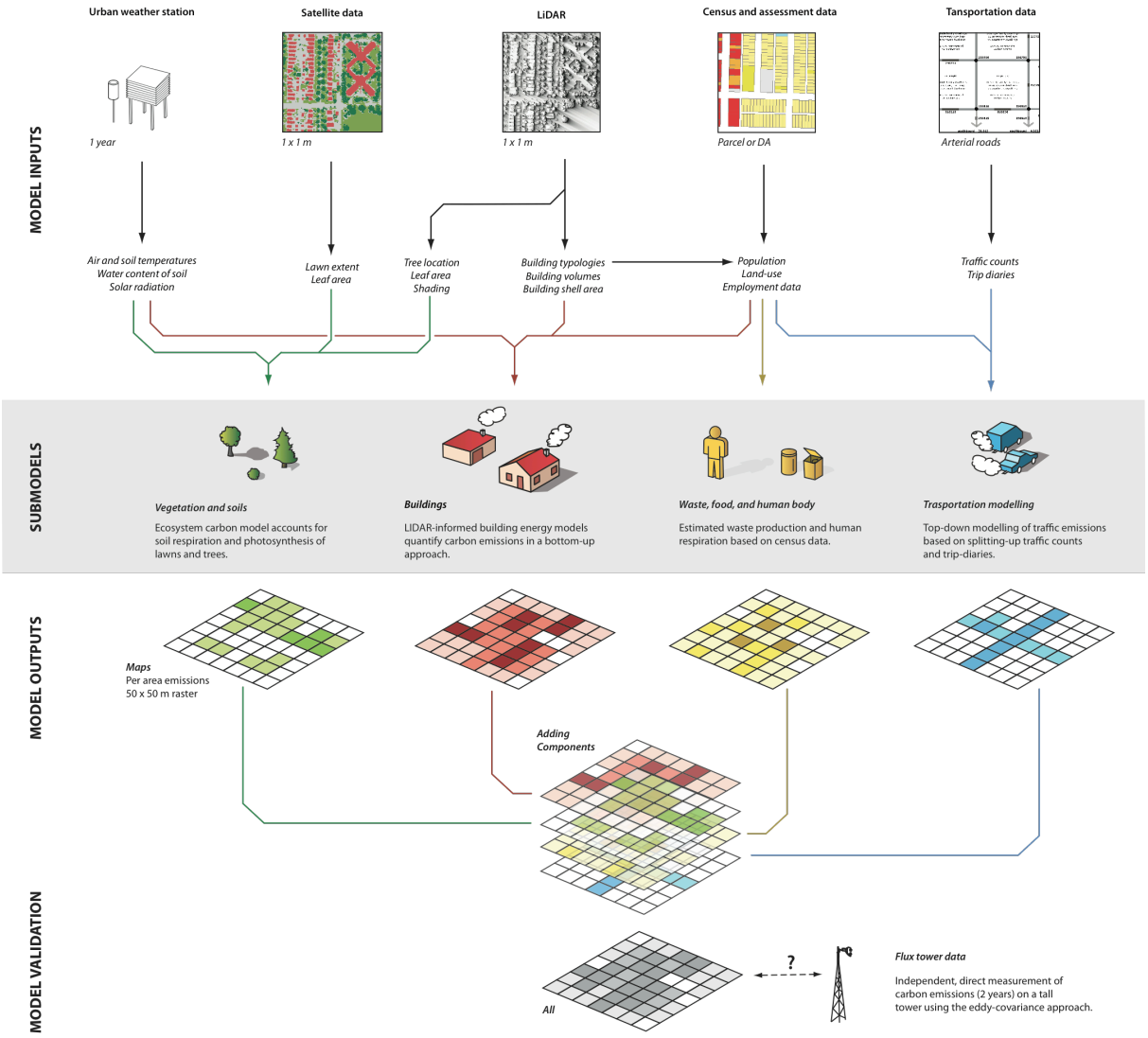

Fig. 1 - *Diagrammatic representation of emission modeling approach. At the centre (grey band) are the four metabolism components or sub-models — vegetation and soils, buildings, human metabolism and transportation. At the top, are the data sources from which sub-model inputs are derived and aggregated. Below are model outputs which are modeled carbon emissions estimates expressed in quantitative (how much) and spatial (where) terms. At the bottom is the model validation step against EC measurements.*

processes that convert between carbohydrates and CO_2, namely combustion, respiration, and photosynthesis. In this contribution we are solely interested in those vertical fluxes – as vertical fluxes can be measured using micrometeorological flux measurements on towers. Those vertical fluxes are CO_2 emissions from fossil fuels, but also include respiration and uptake by urban vegetation.

The spatial modeling of emissions is conceptually separated into four components (buildings, transportation, human respiration and vegetation/soils) that are illustrated along with model inputs in Fig 1. Recent advances in remote sensing technology have significantly improved the accessibility and accuracy of high resolution, site-specific spatial data. In the current study, we make extensive use of high resolution Light Detection and Ranging Data (LiDAR, 1 m resolution) and multi-spectral satellite data (Tooke et al. 2009). Based on those fine-scale inputs, which are available for the entire study area, for each component spatial maps of total annual CO_2 emissions (or uptake) are created at 50 m resolution. Those four maps are then summed to create a map of total emissions at 50 m resolution (Fig 1, bottom). The modeling approach of each of the sub-models is described in sections 2.2 to 2.5 and a more detailed description can be found in Christen et al. (2010, in press).

2.2 Emissions from Buildings

This component includes stationary combustion sources transforming fossil fuel carbon (natural gas, oil, coal) or renewable carbon (wood fires) into CO_2 for space heating or cooling, hot water, lighting, space cooling, auxiliary equipment loads and industrial processes. Building construction, morphology, building use, and urban density all influence energy demand, and ultimately CO_2 emissions released into the atmosphere.

Building typology approach - A bottom-up building-typology approach was used to describe the study neighborhood through a series of building prototypes that are characteristic of the existing building stock. Through fieldwork and a synthesis of precedent work, two overarching building categories emerged for the study area (residential and 'other,' non-residential) along with thirteen sub-types. Of the 4558 buildings sampled in the Sunset neighborhood, 95% were residential, a significant percentage necessitating a more rigorous categorization. Residential buildings were further divided based on form (stacked, detached and attached), resulting in four additional categories: apartments, row houses, duplexes and single family detached (SFD). Of the total number of residential building in the study area 97% are SFD that were further divided in three sub-types based on year of construction. Additionally, a significant proportion of these SFD classes have secondary suites and thus each sub-type was assigned a derivative. These derivatives were modeled with larger occupancies and adjusted morphological and system attributes accordingly. The typology concept focuses on building attributes relevant to energy consumption; these include (a) morphological attributes of buildings, such as heated volume, and window, wall and roof areas (b) energy performance attributes such as heating system types and thermal resistance values. These attributes, along with building use were identified as key energy performance indicators and formed the basis of the building typology categorization.

Building energy modeling - To estimate CO_2 emissions two building energy models (BEM), one dedicated to ground oriented residential sub-types (HOT2000) and one for 'other' building types (OEE Screening tool) were used. HOT2000 has undergone extensive validation (Haltrecht and Fraser, 2000) and is primarily used in performance evaluation programs by researchers, utilities and governmental agencies. In order to provide HOT2000 with locally relevant inputs for Sunset neighborhood several steps were taken to extract the morphological and performance attributes from LiDAR data and associated with a heated floor area and representative models created in a 3D modeling software. The morphological characteristics from this model, where matched to the sub-type characteristics from the LiDAR data.

CO_2 emissions from the building sector - In the study area, a large part of residential energy use is dedicated to space heating, of which the majority is powered by natural gas which has a emission factor of 13.9 kg C GJ^{-1}. Electricity, another significant source of building energy, typically provides power for building lighting, auxiliary equipment and space cooling or may entirely replace natural gas as the primary source of heating energy. CO_2 emissions resulting from electricity production are significantly less than natural gas due to the large proportion of hydroelectric power in British Columbia, and the emission factor is 1.67 kg C GJ^{-1} (BC GHG Assessment Guide, 2008).

Results - 2.47 kg C m^{-2} $year^{-1}$ are locally emitted from buildings with 2.15 kg C m^{-2} $year^{-1}$ modeled from residential buildings and 0.32 kg C m^{-2} $year^{-1}$ from commercial and institutional ones. The spatial distribution of building emissions can be seen in Fig 2a. Those numbers only include local emissions due to natural gas combustion, i.e. release of CO_2 outside the study area due to power generation was modeled, but is not considered here – as those emissions would not be measured on the tower.

2.3 Emissions from Transportation

Mobile combustion sources transform fossil fuels (gasoline, diesel) into CO_2. The challenge with estimating the magnitude of this component is accounting for the extreme variation of sources in space and time. The goal of the transportation submodel is to estimate the fossil fuel combustion that happens locally in the study area by vehicle trips to, from and through the study area.

Traffic count data - Within the project study area were 13 directional traffic count sites with one or more sets of recent (since 2005) 24-hour weekday traffic counts and nine intersection traffic movement counts with a few hours of peak travel data. Data gathered at these points were used to construct a weekday traffic profile. In this profile all vehicle trips were assumed to enter or exit the study area along one of the arterial roads for which counts were available. According to the Ministry of Transportation and Greater Vancouver Transportation Authority (2004) average trip rates and mode splits in the City of Vancouver are 3 trips per day and capita, 0.605 of which are by automobile. These rates were used to estimate the local trip share as 24% and through trips at 76% of total trips.

CO_2 emissions from the transportation sector - emissions from transportation sources depend on vehicle type and the associated fuel efficiency. Trips by vehicle were estimated using four-type types: light vehicles, transit vehicles, medium freight vehicles, and heavy freight vehicles. At one intersection at the northern centre of the study area a vehicle class traffic count was available and is used to estimate vehicle classes on arterials. Average fuel efficiencies and conversion factors (NRCan, 2007) were used to estimate the amount of fuel combusted and CO_2 emitted for each trip and vehicle type within the study area.

Results – In the study area, 2.93 kg C m^{-2} $year^{-1}$ are emitted from the transportation sector. It is evident from the map in Fig 2b that arterial roads are emission 'hot spots', where, on a relatively small area, significant emissions are released. Out of all transportation emissions, only 11% (0.31 kg C m^{-2} $year^{-1}$) are attributable to trips within the study area with the remainder (89%; 2.62 kg C m^{-2} $year^{-1}$) to trips passing through the study area.

2.4 Emissions due to human respiration

This component includes CO_2 emissions by the human metabolism. The carbon cycled through this component is entirely renewable (food) and does not provide opportunities for emission reductions, however CO_2 emitted by human respiration is measured on the tower, and hence it was

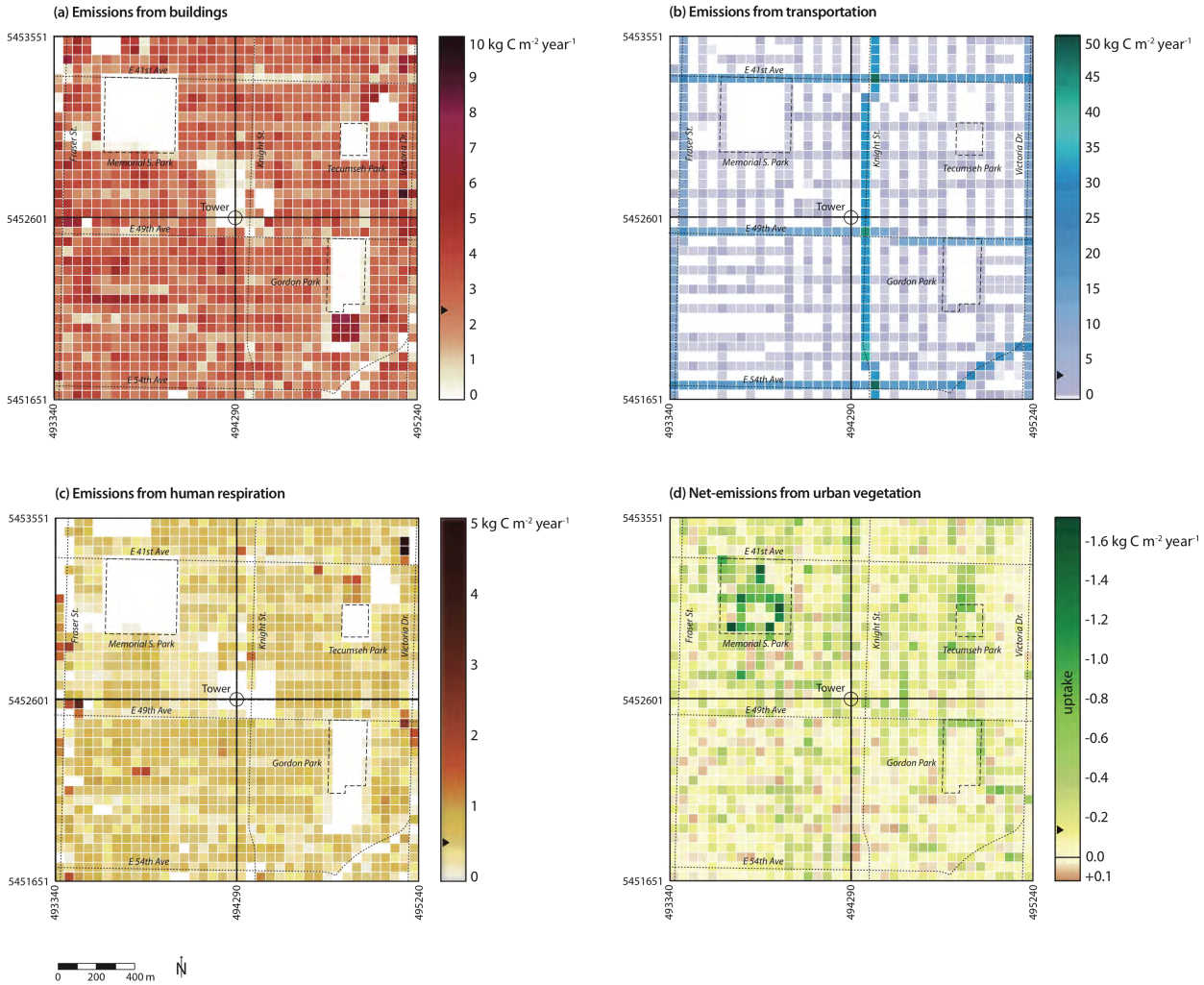

Fig. 2 – *Raster maps of annual total (local) CO_2 emissions at 50 m grid resolution for (a) buildings, (b) transportation, (c) human respiration and (d) vegetation. Negative numbers for vegetation indicate uptake. Note the different scales.*

included in the modeling approach as a flux into the atmosphere.

CO_2 emissions due to human respiration - The injection of CO_2 by human respiration into the atmosphere was calculated using detailed night-time population distribution (based on census data and distributed using LiDAR and land-use data). Based on the typical annual respiration of a human body in 76.3 kg C year^{-1} cap^{-1} (Moriwaki and Kanda, 2002), the CO_2 emission due to human respiration was estimated as 0.49 kg C m^{-2} year^{-1}. The spatial distribution can be seen in Fig 2c.

2.5 Emissions and uptake by vegetation and soils

This component can act as sink or source through photosynthesis and respiration. As it entirely involves renewable carbon it is not accounted for in most studies related to urban sustainability. However, the ability of urban vegetation to sequester fossil fuel carbon in urban biomass and soils make this component relevant in urban metabolism studies. Moreover, indirect effects of urban vegetation (shading, sheltering) can reduce / increase energy demands for space heating and cooling. Indirect effects are included in the building energy sub-component (section 2.2).

CO_2 emissions from soils, lawns and trees - Respiration from soils and lawns was modeled based on empirical relations derived from approx. 280 closed-chamber measurements with an opaque chamber on representative residential laws in the study area. Respiration was modeled for 5-min steps over a full annual cycle as a function of soil temperature and volumetric water content following Liss et al. (2009). Inputs used were direct and continuous observations of soil volumetric water content and soil temperatures on four residential lawns in the study area. Lawn fraction was extracted from remote sensing data following Tooke et al. (2009). Extensive and regular lawn irrigation was shown to control annual soil respiration by a factor of two. Lawn respiration

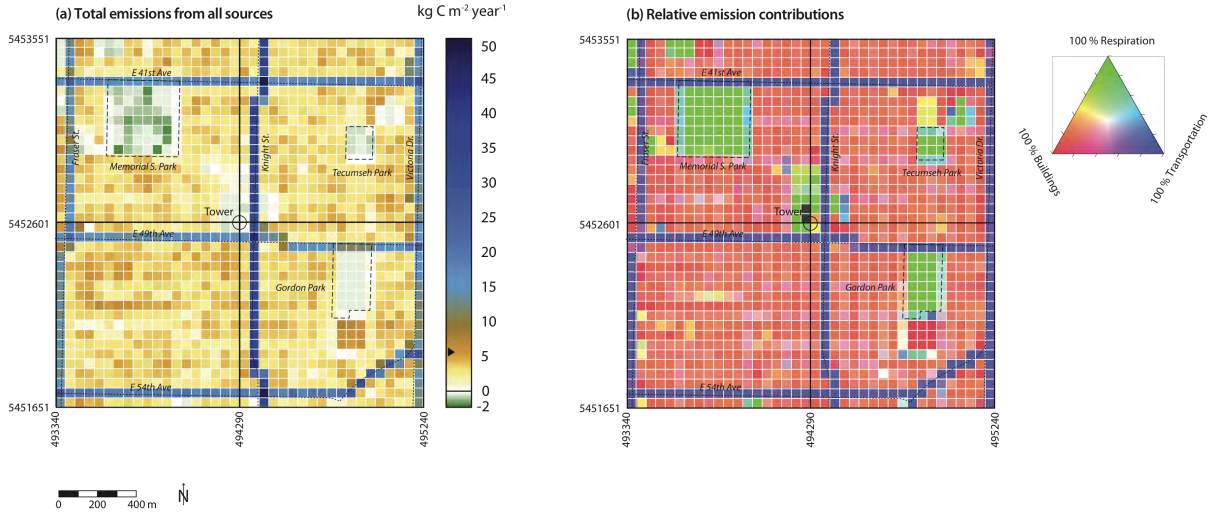

Fig. 3 – *Raster maps of (a) annual total (local) CO_2 emissions from all sources and (b) RGB composite map of relative contributions of local CO_2 emission sources – buildings (red), transportation (blue) and respiration (green, human and soil respiration combined) to the total emissions from each raster cell.*

ranged between 0.81 kg C m^{-2} (lawn) $year^{-1}$ for properties with no irrigation and 1.79 kg C m^{-2} (lawn) $year^{-1}$ for properties with regular and extensive lawn sprinkling.

Respiration from above-ground biomass was modeled based on measurements from a portable photosynthesis measurement system (Li-6400, Licor Inc., Lincoln, Nebraska, USA) on a total of 12 urban trees and shrubs in the study area. Above-ground respiration was scaled up from leaf to neighborhood using a LiDAR derived leaf area index and year-round climate data. Respiration from above-ground biomass was integrated in 5-min steps over a full annual cycle for the year 2009.

Results for respiration - The neighborhood-wide emissions due to soil and lawn respiration were calculated as 0.28 g C m^{-2} $year^{-1}$. This value includes autotrophic respiration of lawns and tree roots. Autotrophic above-ground respiration of trees was estimated as 0.05 kg C m^{-2} $year^{-1}$. The sum of soil lawn and tree respiration was 0.33 g C m^{-2} $year^{-1}$ and contributes 5% to all local emissions (but is offset by photosynthesis).

CO_2 uptake by photosynthesis - Photosynthesis of urban lawns was modeled based on empirical relations derived from closed-chamber measurements with a clear chamber and co-located photosynthetically active radiation (PAR) sensor over representative lawns in the neighborhood. Photosynthesis of lawns was modeled based on PAR irradiance (Ogren and Evans, 1993) taking into account shading and reduction if photosynthetic activity due to water stress by low soil volumetric water content in summer. For 5-min steps, PAR irradiance of was estimated on a 1 x 1 raster for all lawn surfaces in the neighborhood based on measured short-wave irradiance above the canopy. Photosynthesis by trees was modeled based on measured light-response curves from 12 representative trees in the neighborhood that were combined with a simple multi-layer radiation transmission at 1 m^3 resolution. Similarly to the lawn photosynthesis model, the tree photosynthesis model was driven by measured short-wave irradiance and additional climate data for the whole year of 2009.

Results for photosynthesis – CO_2 uptake by photosynthesis was found to be -0.21 kg C m^{-2} $year^{-1}$ for lawns and -0.28 kg C m^{-2} $year^{-1}$ for trees, resulting in a direct net sequestration of 0.33 (respiration) – 0.49 (photosynthesis) = -0.16 kg C m^{-2} $year^{-1}$. Note that part of the CO_2 taken up (0.07 kg C m^{-2} $year^{-1}$) is laterally exported due to removal of litter, clippings etc., so actual sequestration is reduced to -0.09 kg C m^{-2} $year^{-1}$.

2.6 Total emissions

The summed local emission components (buildings, transportation, human metabolism, and vegetation/soils) are shown in Figure 3a. From a total of 5.74 kg C m^{-2} $year^{-1}$ in the study area, 40% are originating from buildings, 47% from transportation, 8% from human respiration and 5% from respiration of soil and vegetation. Those are partially offset by an annual uptake of -9% though photosynthesis of urban vegetation (lawns and trees). Out of the local *fossil fuel emissions* in the study area, 46% originate from the building sector, whereas 54% are from the transportation sector. 51% of all local fossil fuel emissions are of local origin, 49% are from through traffic.

Figure 3b illustrates for each 50 m raster element the relative contribution from three major emission sectors (buildings in red, transportation in blue, and respiration in green). Respiration is the sum of human respiration, soil respiration and vegetation respiration but does not include CO_2 uptake by photosynthesis. In the majority of the area, buildings are the dominant source (midblock) with the exception of arterial roads (transportation) and parks (respiration).

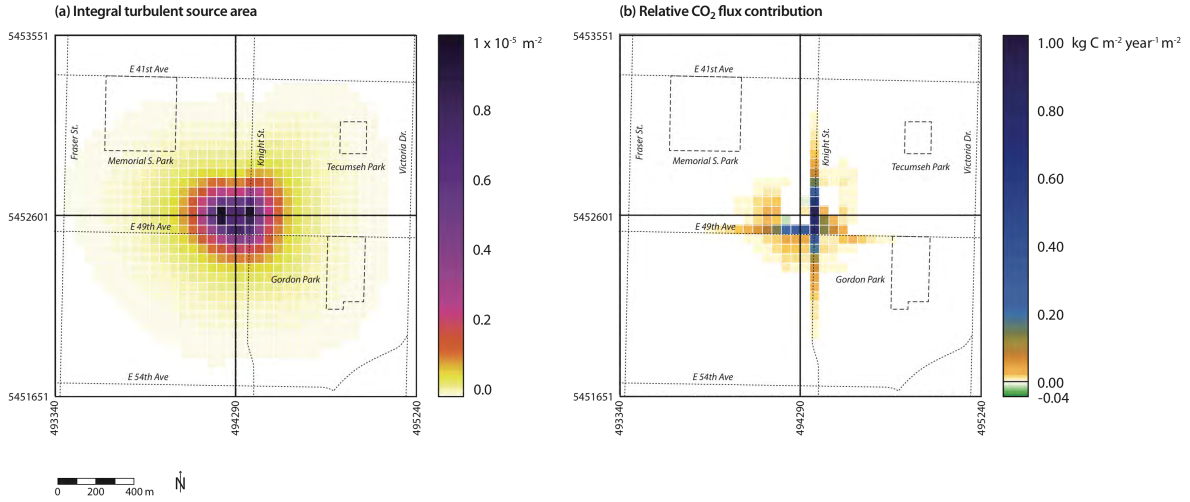

Fig. 4 – *Raster maps of (a) integral turbulent source area for the period May 1, 2008 to April 30, 2010 (b) source-area weighted CO_2 fluxes (flux-contributions, product of maps Fig 4a and Fig 3a).*

3 DIRECT CO_2 FLUX MEASUREMENTS

3.1 Site, instrumentation and processing

Site and instrumentation - The EC system used in this study is located in the centre of the chosen study area on a tower 28.8 m above the local ground surface The Vancouver-Sunset neighborhood was identified as a flat and homogeneously developed area when the research site was chosen in 1978 (for primarily energy balance studies) – However for CO_2, model results suggest that the homogeneity hypothesis does not hold and a more detailed source area attribution is required to aggregate fluxes.

Data used in this study was sampled from May 2008 to April 2010 as part of research in the network 'Environmental Prediction in Canadian Cities'. The instrumentation consists of a sonic anemometer (CSAT 3-d sonic anemometer, Campbell Scientific, Logan, UT, USA) and an open-path infrared-gas analyzer (Li-7500, Licor Inc., Lincoln, NE, USA). Three dimensional wind velocities and CO_2 concentrations are sampled at 20 Hz and are collected on a data logger (CR3000, Campbell Scientific, Logan, UT, USA).

Data processing – Vertical fluxes of CO_2 were calculated as the covariance over 30-minute averaging periods. The coordinate system of the wind velocity components is rotated two times and 30-minute covariances are corrections are applied to account for changes in air density (Webb, et al. 1980) and spatial separation between gas-analyzer and anemometer (Moore 1986). Fluxes undergo several quality control checks, with all details given in Crawford et al. (2010). Using this procedure, 30-minute CO_2 fluxes were calculated for the full 2-year cycle (May 2008 – April 2010). Data coverage for the 2-year period is 70.0% (26.6% of data loss is due to weather, 3.4% due to system failure).

Source areas – The two-year integrated source area of the EC system is shown in Figure 4a. This grid was calculated using a 2-dimensional gradient diffusion and crosswind dispersion model (Kormann and Meixner 2001) that was run for all 30 min periods between May 1, 2008 and April 30, 2010 at a 2 m grid resolution over a domain of 2000 by 2000 m and then upscaled to match the 50 m resolution of the emission maps. Following the procedure described in Chen et al. (2009), the long-term integrated source area was calculated as the average of all individual (changing) 30-min source areas during that period. Approximately 50% of the measured signal is from within approximately 400 m of the tower. This source area is primarily residential and also includes a busy intersection (Knight Street and 49th Avenue).

3.2 Calculation of annual fluxes

Calculation of annual total flux - For annual flux densities, 30-minute fluxes were integrated and spatially sorted to account for different emission characteristics across the source area. Each valid 30-min measurement is sorted by (i) month of the year, by (ii) hour of the day, and by (iii) wind direction (vector average) into one of four sectors (NE (0-90º), SE (90º-180º), SW (180°-270°), and NW (270°-360°). For each month and each wind sector, a typical diurnal course of the flux is then calculated by averaging all situations when wind was from a given sector and within a selected hour. Hours without any occurrence of the wind direction from that sector were linearly interpolated for up to 3 hours. The average diurnal course of that month was then integrated over a full day to retrieve a daily CO_2 flux in g C m^{-2} day^{-1} for each wind sector and each month. For the annual flux density, monthly values from the given sector were integrated and weighted by the number of days in the given month. This procedure was separately applied for weekdays and weekends (as transportation emissions were expected to vary). Flux densities integrated over the entire neighborhood were calculated as the equally weighted, average flux from each of the four wind sectors.

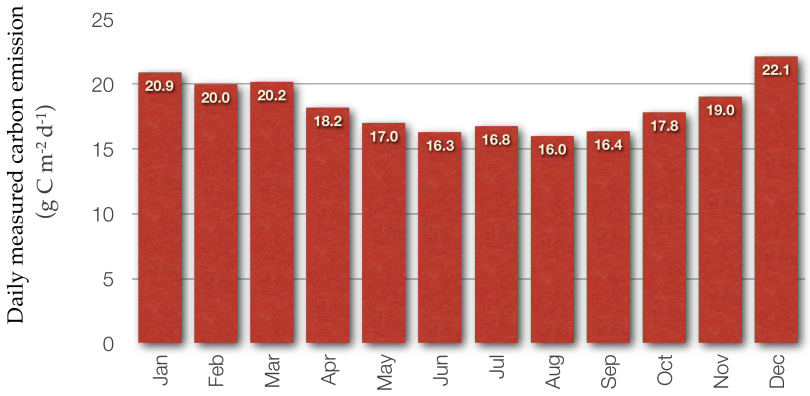

Fig. 5 – *Monthly average CO_2 net-emissions (g C m^{-2} day^{-1}) measured on the flux tower (four equally weighted wind sectors).*

Figure 5 summarizes monthly average CO_2 fluxes in g C m^{-2} day^{-1} for the average of both years. Largest emissions were recorded in the winter months when space-heating requirements are expected to be highest and CO_2 uptake from vegetation is minimal (maximum in December with 22.1 g C m^{-2} day^{-1}). During summer, increased CO_2 sequestration from vegetation is expected, as well as reduced motorized traffic load and no space heating, hence lowering overall measured emissions. The monthly minimum recorded was 16.0 g C m^{-2} day^{-1} in August during school holidays. The annual average was 18.4 g C m^{-2} day^{-1}, which corresponds to 6.71 kg C m^{-2} $year^{-1}$. When stratifying emission measurements into weekends and weekdays, emissions were found always to be lower on weekends for all wind sectors and months, with greatest differences observed for the SE sector (on average 23.8 % weekend emission reduction).

4 COMPARISON OF MEASURED AND MODELLED CO_2 FLUXES

Tables 1 and 3 compare CO_2 fluxes measured on the tower to model results. The model results used for the comparison are aggregated in two different ways. In a simple approach (‘*Radius aggregation’*), all grid cells of the 50m raster that fall within a 400 m radius around the tower are considered and averaged (equally weighted). Those values are then compared to the tower measurements. A 400 m radius was chosen because this corresponds to the 50% source area.

In a more sophisticated aggregation approach, called *‘Source-area aggregation’*, model values are weighted by the turbulent source area. Source areas were calculated for each 30 min step and summed using the same process by which fluxes were aggregated (i.e. for each hour of the day and each month of the year). In this approach, modeled emissions on the 50 m grid were weighted by the spatial source-area distribution (Fig. 4b). A small fraction of the source area (12%) is predicted to be outside the 1900 x 1900 m study area. This fraction was assumed to represent the average flux within the entire study area, assuming that the urban form continues in a similar pattern outside the study area.

4.1 Radius aggregation

For the average of all emissions within a 400-m-radius buffer around the tower, the model results agree very well with the measurements, i.e. 6.71 kg C m^{-2} $year^{-1}$ measured vs. 6.46 kg C m^{-2} $year^{-1}$ modeled. The model slightly underestimates actual emissions by 0.25 kg C m^{-2} $year^{-1}$ (or 4%). With the actual errors associated with the uncertainty of the 400m buffer source area, this is a surprisingly successful result. The model results are split up into different components in Table 2.

The different wind sectors within the 400-m-radius buffer show higher differences, in particular the SE-sector, where measurements are significantly higher (13.16 kg C m^{-2} $year^{-1}$) than modeled values (10.17 kg C m^{-2} $year^{-1}$). This might be an over-proportional contribution of traffic-related emissions from the near-field (intersection 49th Ave. / Knight St. with traffic lights) where both idling and moving vehicles are injecting CO_2 into the atmosphere, but which is not accounted for in the transportation model. In turn, in the two sectors that show arterial road segments without intersections (NE and SW), the model overestimates emissions.

Tab. 1 -*Comparison of modeled and measured carbon emissions for a 400-m-radius buffer around the tower.*

	All	**NE**	**SE**	**SW**	**NW**
Measured flux (kg C m^{-2} $year^{-1}$)	**6.71**	6.57	13.16	4.31	2.81
Modeled flux (kg C m^{-2} $year^{-1}$) aggregated for a 400-m-buffer	**6.46**	7.62	10.17	5.81	2.27
Difference modeled – measured (kg C m^{-2} $year^{-1}$)	**-0.25**	1.05	-2.99	-1.50	-0.54
Difference (percentage)	**-4%**	16%	-23%	35%	-19%

Tab. 2 - *Modeled CO_2 emissions for a 400m buffer around the tower. The total is compared in Tab. 1 against tower flux data.*

	All	NE	SE	SW	NW
Buildings	2.40	2.06	2.67	3.03	1.82
Transportation	3.76	5.29	7.13	2.31	0.35
Human resp.	0.47	0.45	0.51	0.61	0.29
Vegetation, soils	-0.16	-0.18	-0.14	-0.15	-0.19
Total	**6.46**	**7.62**	**10.17**	**5.81**	**2.27**

Tab. 3 - *Comparison of modeled and measured CO_2 emissions weighted by the long-term turbulent source area of the tower.*

	All sectors
Measured flux (kg C m^{-2} $year^{-1}$)	**6.71**
Modeled flux (kg C m^{-2} $year^{-1}$) aggregated by long-term source area	**7.46**
Difference measured – modeled (kg C m^{-2} $year^{-1}$)	**0.75**
Difference (percentage)	**11%**

Tab. 4 - Comparison of measured CO_2 emission reduction on weekends to the modeled transportation sector emissions for a 400-m-radius buffer around the tower. Not enough measurements on weekends with wind from NW were available to estimate the reduction in the NW sector.

	All	NE	SE	SW
Modeled flux density from transportation (g C m^{-2} day^{-1})	**13.15**	14.1	19.1	6.2
Measured difference between weekday-weekend (g C m^{-2} day^{-1})	**5.71**	7.31	9.79	5.59
Weekend reduction to total transportation flux (%)	**42%**	38%	48%	40%

Improving the transportation model and incorporating speed of vehicles in each cell could resolve some of those inaccuracies.

4.2 Source-area aggregation

The source area aggregation is more meaningful than the 400-m-radius buffer method because a significant portion of the measured emissions originate beyond the 400 m boundary. The source areas represent the diminishing contributions of far-field areas rather than applying an abrupt and unrealistic cut-off at 400 m. The source-area aggregated model results are 7.46 kg C m^{-2} $year^{-1}$ (11% higher than the measured 6.71 kg C m^{-2} $year^{-1}$). The source area model combined with the emission model suggests that approximately 70% of all fluxes that were measured at the tower (5.22 kg C m^{-2} $year^{-1}$) originate from transportation (restricted to a narrow part of Knight and 49th Avenue, see Fig. 4b). 27% (2.05 kg C m^{-2} $year^{-1}$) originate from buildings, 5% from human respiration and -2% (-0.17 kg C m^{-2} $year^{-1}$) is offset by vegetation. Although in the entire study area, emissions from buildings and transportation are of approximately equal strength (40% and 47% of all emission, see Section 2.6), the specific location of the tower close to an intersection makes the signal from transportation in the tower signal more relevant. Interestingly, the sector where transportation is small (NW) shows the best agreement between tower and model (2.81 kg C m^{-2} $year^{-1}$ measured vs. 2.87 kg C m^{-2} $year^{-1}$ modeled).

4.3 Weekend-weekday differences

Table 4 compares the observed emission reduction weekday – weekend in three of four sectors to the modeled transportation emissions. The relative emission reduction on weekends (measured, but expressed as fraction of the modeled CO_2 flux from the transportation sector) is estimated as 42%. This suggests that weekend traffic emits 42% less than weekday traffic in the study area.

5 CONCLUSIONS

This study validated a neighborhood-scale CO_2 emission model with directly measured CO_2 fluxes using the eddy covariance approach. Building on a Vancouver case study for which direct flux measurements have been compiled and aggregated, the chosen study demonstrates that methods of integrating diverse emission and uptake processes (combustion, respiration, photosynthesis), on a range of scales converge surprisingly well with directly measured CO_2 fluxes by the EC method on an annual scale. Hence, direct CO_2 flux measurements on urban flux towers are demonstrated to be a method of validation of fine-scale emission inventories / models. Given the errors associated with the uncertainty of the EC-method, the close agreement between tower measurements and model results in this study is a successful and promising outcome. Future research might use temporal (diurnal and seasonal) and spatial (source area) variation to inform further development and refinement of emission models.

Restrictions of the approach - From a conceptual view, it is challenging to define proper system boundaries in an urban ecosystem and flux measurements cannot be used directly to inform planning decisions (but to validate and develop models). If assessing the environmental sustainability of a given urban system, we should consider all processes that are part of the urban metabolism, including effects that take place beyond the city's limits. This conceptual discrepancy between tower measurements and the carbon 'footprint' is summarized in Figure 6. "External emissions due to local activities" refer to the release of CO_2 outside the neighborhood (system boundaries) due to combustion or respiration associated with activities within the neighborhood. "Local emissions due to local activities" refers to the release (or uptake) of CO_2 within the neighborhood (system boundaries) due to combustion, respiration or photosynthesis. "Local emissions due to external activities" - refers to the release of CO_2 within the neighborhood (system boundaries) due to

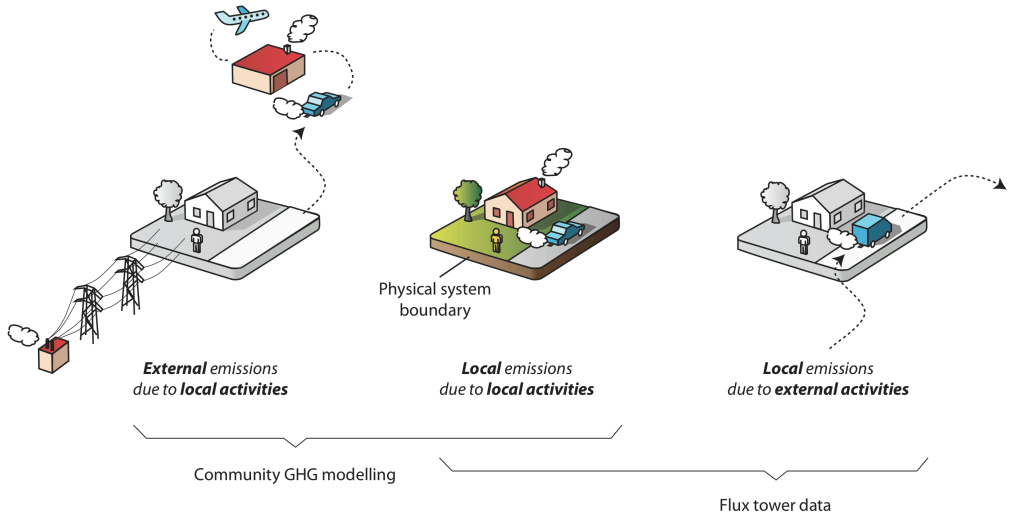

Fig. 6 – *The concept of local and external emissions for a given urban ecosystem. Note the difference between what the tower is measuring and what are deliverables for GHG modeling.*

combustion and respiration from objects or humans travelling through the neighborhood, but not associated with activities in the neighborhood (e.g. through-traffic). Note the difference between what the tower is measuring (local emissions only) and what are deliverables for GHG modeling (emissions due to local activities).

ACKNOWLEDGEMENTS

Principal funding for the modelling project has been provided by CanmetENERGY, Natural Resources Canada, Ottawa (J. Webster, project manager). The Canadian Foundation for Climate and Atmospheric Sciences (CFCAS) funded the acquisition and processing of the LIDAR data as well as the two-year measurements on the flux tower as part of the CFCAS network "Environmental Prediction in Canadian Cities (EPiCC)". Selected research infrastructure on the tower was supported by NSERC RTI (Christen) and CFI / BCKDF (Christen). We acknowledge the support of BC Hydro, the City of Vancouver, Environment Canada and Terasen Gas for providing additional data.

We further acknowledge the significant technical support of staff at the University of British Columbia including (in alphabetical order): J. Bau, E. Heyman, R. Ketler, Z. Nesic, J. Ranada, C. Siemens.

REFERENCES

Baker, N., & Steemers, K. (2000): 'Energy and Environment in Architecture: A Technical Design'. New York: E&FN Spon.

Chen, B., Black, T.A., Coops, N.C., Hilker, T. Trofymow, J.A., Morgenstern, K. (2009): 'Assessing tower flux footprint climatology and scaling between remotely sensed and eddy covariance measurements'. *Boundary-Layer Meteorol.* 130 (2), 137-167.

Christen A., Coops N., Kellett R., Crawford B., Olchovski I., Tooke R., van der Laan M. (2010): 'A LiDAR-Based Urban Metabolism Approach to Neighbourhood Scale Energy and Carbon Emissions Modelling' – Technical Project Report, University of British Columbia.

Crawford, B. Christen A., Ketler R. (2010): 'EPiCC Technical Report 1: Processing and quality control procedures of turbulent flux measurements during the Vancouver EPiCC experiment'. http://www.geog.ubc.ca/~epicc/reports/Vancouver-EPiCC-Tech-Report-1.pdf

Haltrecht D., and Fraser K. (1997): 'Validation of HOT2000 using HERS BESTEST' IBPSA

Kormann, R. and F.X. Meixner (2001): 'An analytical footprint model for non-neutral stratification'. *Boundary-Layer Meteorology* 99, 207-224.

Moore, C.J. (1986): 'Frequency response corrections for eddy correlation systems'. *Boundary-Layer Meteorology*, 37, 17-35.

Moriwaki R., Kanda M. (2004): 'Seasonal and diurnal fluxes of radiation, heat, water vapor, and carbon dioxide over a suburban area'. *J. Appl. Meteorol.* 43, 1700-1710.

Province of British Columbia. 'BC GHG Emissions Assessment Guide'

Salat, S. (2007): 'Energy and Bioclimatic Efficiency of Urban Morphologies: Towards a Comparative Analysis of Asian and European Cities'. In Proceedings of the International Conference on Sustainable Building Asia (pp. 161-166). Seoul: Fraunhofer IRB.

Tooke, R., Coops, N.C., Goodwin, N.R., & Voogt J.A. (2009): 'The influence of vegetation characteristics on spectral mixture analysis in an urban environment'. *Remote Sensing of Environment*, 113, 398-407

Walsh, C.J. (2005): 'Fluxes of radiation, energy, and carbon dioxide over a suburban area of Vancouver, BC'. M.Sc. Thesis, Department of Geography, University of British Columbia.

Webb, E.K., G.I. Pearman, and R. Leuning (1980): 'Correction of flux measurements for density effects due to heat and water vapour transfer'. *Quarterly Journal of the Royal Meteorological Society*, 106, 85-100.